IEEE Access
Multidisciplinary | Rapid Review | Open Access Journal

Received January 10, 2020, accepted January 16, 2020, date of publication February 18, 2020, date of current version February 25, 2020.

Digital Object Identifier 10.1109/ACCESS.2020.2972039

Ungrounded Coplanar Waveguide Based Straight Line Methods for Broadband and Continuous Dielectric Characterization of Microwave Substrates

LONGZHU CAI, (Member, IEEE), ZHI HAO JIANG, (Member, IEEE), YAN HUANG, (Member, IEEE), AND WEI HONG, (Fellow, IEEE)
State Key Laboratory of Millimeter Waves, School of Information Science and Engineering, Southeast University, Nanjing 210096, China

Corresponding author: Longzhu Cai (longzhu.cai@seu.edu.cn)

This work was supported in part by the National Natural Science Foundation of China under Grant 61901108 and Grant 61901112, in part by the Natural Science Foundation of Jiangsu Province, China, under Grant BK20180364, in part by the Fundamental Research Funds for the Central Universities under Grant 3204009409, and in part by the Jiangsu Province Double Innovation Project under Grant 1104000376.

ABSTRACT This work presents a novel method for fast characterization of broadband and continuous dielectric properties of microwave substrates based on an ungrounded coplanar waveguide (UGCPW) structure containing two simple straight lines. The proposed method could, to some extent, alleviate the derivation error due to connector soldering and device fabrication. To verify this point, theoretical analysis and result comparisons are carried out. By considering both the conductor loss and radiation loss, the dielectric loss tangent can be retrieved with a high precision. The deviation of the measured dielectric constant and dielectric loss tangent are found to be within 0.03 (0.68%, 4.37 vs 4.40) and 0.0013 (6.5%, 0.0213 vs 0.02), respectively, in the range from 12 to 20 GHz, which is more accurate than the results reported in the literature, all while the proposed extraction approach is simpler than other methods such as the wave cascading matrix (WCM) algorithm. Due to the UGCPW configuration, this method is suitable for property evaluation of emerging synthesized dielectric materials, as a single round of electroplating process is required for device design, which can eliminate possible consistency error in conductor thickness and roughness caused by multiple electroplating process.

INDEX TERMS Dielectric properties, ungrounded coplanar waveguide (UGCPW), dielectric constant, dielectric loss tangent, FR4.

I. INTRODUCTION

Before designing microwave devices, it is crucially important to accurately understand the dielectric properties of the used substrate materials, especially their dielectric constants. However, most printed circuit board (PCB) manufacturers usually provide dielectric information only at a single frequency, e.g. 1 GHz. Hence, any dielectric constant deviation may result in frequency shift if the inaccurate dielectric information is used during the design process. In addition, modern microwave dielectrics are not only limited to conventional hard ceramic laminates, but also encompass non-traditional flexible materials such as fabric substrates and newly developed dielectric materials [1]–[7]. Therefore, the accurate characterization of material dielectric properties is of significant importance, thus has been naturally drawing extensive attention.

In general, there are different kinds of methods and techniques for measuring the material properties at microwave frequencies, but none of them is suitable for all different types of substrate materials in the entire frequency spectrum. The measurement techniques have to be selected according to the estimated dielectric properties of the materials under test (MUT), such as the material size and state, the required extraction accuracy, the processing simplicity, the bandwidth of interest, as well as the required type of testing equipments [4], [8]–[16]. The material characterization techniques can be divided into two main categories based on bandwidth, namely *broadband measurement* and *narrowband measurement* [17]. The narrowband measurement primarily relies

The associate editor coordinating the review of this manuscript and approving it for publication was Kuang Zhang.

on resonant cavities with more accurate results, but only at discrete resonant frequencies [9], [18], [19]. The broadband technique is typically based on the complex transmission and/or reflection coefficients of electromagnetic waves propagating within the MUT with a non-resonant structure [17]. The merit of the broadband measurement technique is that it can obtain a broadband material property, while it owns a lower extraction accuracy [10]. There are two kinds of broadband measurement techniques - guided-wave structure based technique and space-wave structure based technique.

One of the broadband measurement techniques by applying the guided-wave structure is defined as multiline method, which was developed in 1991 to improve the extraction accuracy and bandwidth over conventional thru-reflect-line (TRL) method [20]. In this method, a third line was employed such that the propagation constant can be determined with a better accuracy. After that, an optimized error correction method was proposed by applying only two non-reflecting transmission lines instead of a complete set of calibration standards (at least three steps), in which the wave cascading matrix (WCM) was used for minimizing the error [21]. In 2019, the dielectric material characterization of plastic filaments used for 3D printing was investigated by the multiline method, in which the WCM method was applied as well. A rectangular coaxial transmission-line fixture was employed, and the MUT was placed inside the coaxial fixture. However, due to the conducting loss of the fixture, the extraction error percentage of dielectric constant and loss tangent could be as large as 5% and 10%, respectively [10]. The effective dielectric constant of an unknown substrate can also be derived based on the phase difference of two microstrip line configurations, which is another type of guided-wave structures [22]. However, the substrate dielectric constant and loss tangent were not analyzed and calculated.

For the space-wave structure based broadband measurement, one example is to extract the effective parameters of planar metamaterial slabs by applying the WCM method. The broadband effective material parameters of metamaterial slabs determined in the range from 5 to 15 GHz was investigated by comparing the scattering parameters of the metamaterial slabs with different thickness values and distances away from the horn antennas [23]. But the shortcoming of such method is that the size of slabs needs to be electrically large, and the measurement accuracy is sensitive to the relative location between the slabs and transmitting/receiving antennas. It can be seen from the above literature that these methods possess certain deficiency in the calculation of dielectric properties. For instance, dielectric materials need to be filled in coaxial transmission lines, which are widely used, but are also expensive to produce and time consuming to measure [20]. In addition, the WCM algorithm is usually applied for calculation and the extraction accuracy needs to be further improved due to the influence of other losses [10]. Finally, the multiline methods have not been intensively studied in microstrip line or coplanar waveguide structures.

In this work, we propose an optimized method based on the ungrounded coplanar waveguide (UGCPW) configuration with two simple straight lines for fast characterizing dielectric materials at microwave frequencies. The UGCPW structure is very suitable for electroplating certain newly developed dielectric materials, avoiding high fabrication cost and difficulty, as well as possible consistency error in conductor thickness and roughness caused by multiple electroplating process, e.g. at least two electroplating steps are required for the upper and lower layers of a microstrip configuration. Furthermore, this method can offer broadband and continuous dielectric parameter extractions. The error due to connector soldering and fabrication could also be alleviated to a certain extent. Without using the WCM algorithm, the transmission magnitudes and phases are enough for material property extraction. By considering various losses associated with the UGCPW structure, including the conductor loss and radiation loss, the extraction accuracy of the proposed method is greatly improved.

II. PROPOSED METHOD AND THEORY

For a UGCPW based simple straight line with a length of L, the effective dielectric constant ε_{eff} of the substrate can be obtained through its transmission (S_{21}/S_{12}) phases $\emptyset$ (in degrees) as

$$\emptyset = \frac{L \times f \times \sqrt{\varepsilon_{eff}(f)} \times 360^{\circ}}{c}, \tag{1}$$

$$\varepsilon_{eff}(f) = \left(\frac{\emptyset \times c}{L \times 360^{\circ} \times f}\right)^{2}, \tag{2}$$

where c is the speed of light in vacuum, and f is the working frequency.

However, the transmission phase $\emptyset$ may have a certain deviation due to the influence of connectors, soldering, and fabrication inaccuracy, which would inevitably result in errors in the extracted effective dielectric constant and also substrate dielectric constant. Such error also occurs in the retrieved substrate dissipation factor as well. To tackle with this problem, we propose an optimized method with two UGCPW straight lines to reduce the error caused by the factors mentioned above, which can increase the reliability of the obtained substrate dielectric constant ε_r and the dissipation factor $\tan\delta$ (defined as the imaginary part of complex permittivity over the real part of complex permittivity). Figure 1 shows a schematic diagram of the structure used in the proposed method for MUT, and the related parameters will be described in the following sections.

For UGCPW straight lines with lengths of L_{Long} and L_{Short}, assuming their corresponding transmission phases are $\emptyset_{Long}$ and $\emptyset_{Short}$, respectively. Both the length and phase relations can be expressed as follows when X is used to represent either the length L or the phase $\emptyset$,

$$2X_{error} + X_{Long\_M} = X_{Long}, \tag{3}$$

$$2X_{error} + X_{Short\_M} = X_{Short}, \tag{4}$$

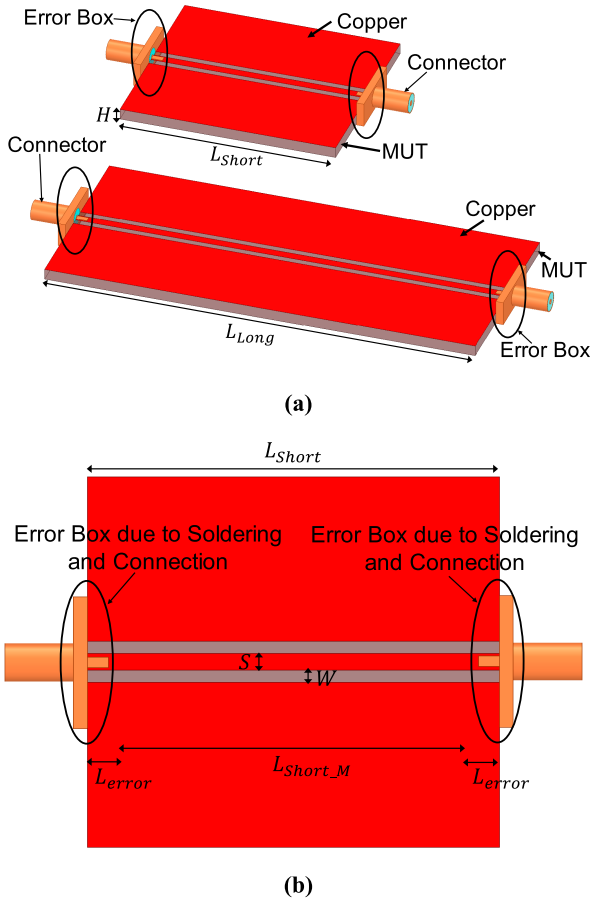

FIGURE 1. Schematic diagram of the proposed method. (a) UGCPW straight lines with length L_{Long} and L_{Short}; (b) top view of the zoomed in UGCPW straight line with length L_{Short}, showing the error box due to soldering and connection.

thus

$$X_{Long\_M} - X_{Short\_M} = X_{Long} - X_{Short}. \tag{5}$$

In the above equations, L_{Long_M} and L_{Short_M} are the lengths of the middle section, by removing the effect of SMA connecting and soldering issues which is expressed by length error L_{error} and phase error $\emptyset_{error}$. In the next step, the ideal relation of phase ($\emptyset$) and length (L) described in equations (1)-(2) can be applied to calculate their phase difference as follows:

$$\emptyset_{Long\_M} - \emptyset_{Short_M} = \frac{(L_{Long\_M} - L_{Short_M}) \times f \times \sqrt{\varepsilon_{eff}(f)} \times 360^{\circ}}{c} \tag{6}$$

By combining equations (5) and (6), the following relation with less connection/soldering errors is obtained:

$$\varepsilon_{eff}(f) = \left(\frac{(\emptyset_{Long} - \emptyset_{Short}) \times c}{(L_{Long} - L_{Short}) \times 360^{\circ} \times f}\right)^2. \tag{7}$$

It should be mentioned that the above derivation is based on the assumption that the connection and soldering of the long and short lines are identical. Once the effective dielectric constant $\varepsilon_{eff}(f)$ is known, the substrate dielectric constant ε_r can be derived by the following expression [24]

$$\varepsilon_r = 1 + \frac{\varepsilon_{eff} - 1}{q}, \tag{8}$$

where the filling factor q is given by

$$q = \frac{\mathrm{K}(k_1)/\mathrm{K}(k_1')}{2\mathrm{K}(k_0)/\mathrm{K}(k_0')}. \tag{9}$$

K is the complete elliptic integral of the first kind, k_0' and k_1' are the complementary moduli associated with the modulus k_0 and k_1, and they are given by

$$k_0 = \frac{S}{S + 2W}, \tag{10}$$

$$k_1 = \sinh(\pi S/4H)/\sinh\left(\frac{\pi (S + 2W)}{4H}\right), \tag{11}$$

$$k_i' = \sqrt{1 - k_i^2} \quad (i = 0, 1), \tag{12}$$

where S and W are the signal line width and gap of the UGCPW structure, respectively, and H is the substrate thickness. The ratio $K(k)/K(k')$ can be evaluated by

$$\frac{K(k)}{K(k')} = \frac{K(k)}{K'(k)} = \frac{1}{\pi}\ln\left(2\frac{1 + \sqrt{k}}{1 - \sqrt{k}}\right) \quad 0.7 \le k \le 1, \tag{13}$$

$$\frac{K(k)}{K(k')} = \frac{K(k)}{K'(k)} = \left[\frac{1}{\pi}\ln\left(2\frac{1 + \sqrt{k'}}{1 - \sqrt{k'}}\right)\right]^{-1} \quad 0 \le k \le 0.7. \tag{14}$$

The above expression $K(k)/K(k')$ possesses an accuracy of one part in 100000, and the values of $K(k)$ and $K'(k)$ parameters can also be worked out [24].

The transmission magnitude of UGCPW straight lines can be obtained directly, which is related to the total attenuation α_t. The conductor loss α_c of a UGCPW straight line is associated with the characteristic impedance Z_0 and is known as [24]–[26]

$$\alpha_c = \frac{20}{\ln 10}\frac{R_c + R_g}{2Z_0}, \tag{15}$$

$$Z_0 = \frac{30\pi}{\sqrt{\varepsilon_{eff}(f)}\left(\frac{\mathrm{K}(k_0)}{\mathrm{K}(k_0')}\right)}, \tag{16}$$

where R_c is the distributed series resistance of center strip conductor in ohms per unit length and R_g is the distributed series resistance of ground planes in ohms per unit length. Note that the unit of the conductor loss α_c in equation (15) is in decibels per unit length instead of Nepers per unit length.

Although the attenuation due to radiation in the proposed UGCPW structures is very small since the straight-line structure has no discontinuities, it is still should be analyzed and included in the calculation in order to obtain more accurate results. The radiation loss α_r is related to the dielectric wavelength λ_d, which can be obtained by [27]

$$\alpha_r = f(\varepsilon_r)\left(\frac{1}{\lambda_d}\right)^3 \frac{(S + 2W)^2}{K(k_0)K'(k_0)}, \tag{17}$$

where the expressions of the radiation form factor $f(\varepsilon_r)$ is given by

$$f(\varepsilon_r) = \left(\frac{\pi}{2}\right)^5 \frac{1}{\sqrt{2}} \frac{\left(1 - \frac{1}{\varepsilon_r}\right)^2}{\sqrt{1 + \frac{1}{\varepsilon_r}}}, \tag{18}$$

The conductivity of most dielectrics is extremely low, hence the resulting attenuation is usually very small. In our calculation, the loss due to the substrate conductivity term was ignored. Therefore, the dielectric loss α_d in UGCPW straight lines can be calculated according to

$$\alpha_d = \alpha_t - \alpha_c - \alpha_r. \tag{19}$$

By optimizing the difference of transmission magnitude between the long and short UGCPW straight lines, the attenuation errors due to the connection and soldering can be minimized as well, which can be expressed as

$$\alpha_t = \frac{-(|S_{21}|_{Long} - |S_{21}|_{Short})}{L_{Long} - L_{Short}}. \tag{20}$$

Once the dielectric loss α_d is obtained, the dissipation factor $\tan\delta$ of the dielectric material can be calculated by [24]

$$\tan\delta = \frac{\alpha_d c \sqrt{\varepsilon_{eff}}}{q \varepsilon_r f \pi} \frac{1}{\frac{20}{\ln 10}}. \tag{21}$$

In this method, the error mainly comes from the inaccuracy of the formulas calculating characteristic impedance Z_0 and conductor loss α_c, the inaccuracy of manufacturing dimensions, and the inconsistent connectors and soldering situation. The formulas of calculating Z_0 and α_c in this algorithm are based on quasi-transverse electromagnetic (TEM) approximation, which can be obtained by conformal mapping method [24]. Errors could occur when the quasi-TEM approximation is not valid. In the manufacturing process, the device dimensions may have deviation, which will also lead to the error in the extracted parameters. For the error caused by inconsistent connectors and soldering, the proposed method assumes that the connectors and welding situation are completely identical, which is difficult to be the same in practice. Particularly, at high frequencies, the effect of the inconsistency would become more obvious. The specific error analysis will be given in Section III.

III. RESULTS AND DISCUSSION

The widely used substrate material FR4 was employed as the MUT to experimentally verify our method. Two UGCPW straight lines with the lengths of 50 and 100 mm were fabricated, and a photograph of the samples is shown in Fig. 2. The copper with a thickness of 18 um was etched on one side of the 0.5-mm-thick FR4 substrate to form the straight UGCPW structure. The signal line width S and the gap W are 1.3 mm and 0.16 mm, respectively. Two SMA coaxial connectors were carefully soldered on these two UGCPW structures in order to make them have almost the same welding effect to ensure the assumption that their mechanical and electrical properties are identical. The fabricated samples were measured with a vector network analyzer (VNA) N5247A, with the measured transmission scattering parameters depicted in Fig. 3.

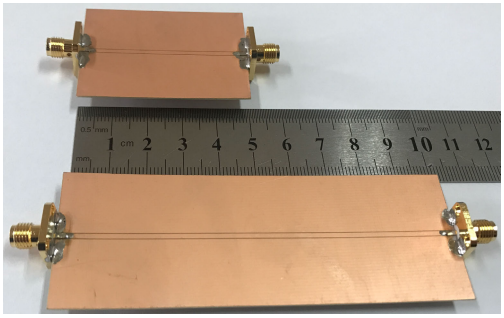

FIGURE 2. Photograph of the fabricated UGCPW straight lines.

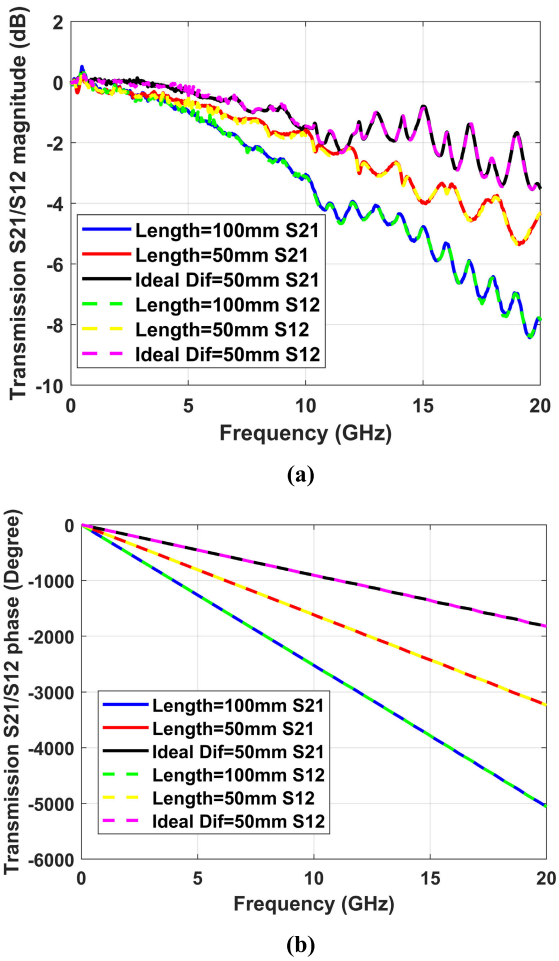

FIGURE 3. The measured transmission S parameters S_{21}/S_{12} of the fabricated UGCPW straight lines with length 100 mm and 50mm, as well as their differential values in (a) magnitude and (b) phase.

It can be seen from Fig. 3 that the magnitude and phase of S_{21} are well matched with those of S_{12} for both structures with lengths of 50 and 100 mm. The transmission phases

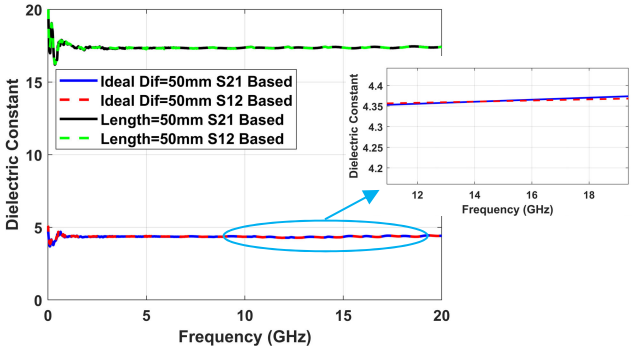

FIGURE 4. The calculated dielectric constants based on the transmission phases of the ideal differential and the fabricated 50-mm-long structures.

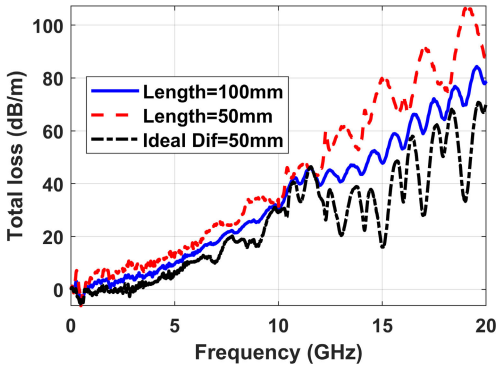

FIGURE 5. The total transmission loss per unit length for the three cases.

in the figure are highly linear. Moreover, the differences between the transmission magnitudes and phases of these two structures are also included in the figure, which can be understood as relatively ideal result of a 50-mm-long UGCPW straight line with reduced effects of SMA connection and welding. When comparing the results of the ideal differential 50-mm-long structure and those of the fabricated one, it can be observed that the transmission phase of the ideal differential 50-mm-long structure is smaller. This might be attributed to the parasitic effect of connector soldering. The corresponding dielectric constants based on the transmission phases of the ideal differential and the fabricated 50-mm-long structures were calculated and compared by using the equation (7) and equation (2), respectively. Using the relationship shown in equation (8) between effective dielectric constant and substrate dielectric constant, the extracted FR4 dielectric constants using these two methods were obtained [see Fig. 4]. It is noticeable that the dielectric constant is around 17.4 when employing the measured data directly from the fabricated straight UGCPW structure, which is dramatically different from the data provided in the vendor's datasheet (dielectric constant and dielectric loss tangent at 10 GHz are 4.4 and 0.02, respectively). However, by applying our proposed method, the calculated dielectric constant is around 4.37, which is fairly close to the value in the datasheet, with a difference of only 0.03, i.e. 0.68%. From this figure, some spikes at low frequencies can be observed, which are probably caused by imperfect calibration during the measurement process [23]. The imperfect calibration at low frequencies can result in inaccurate measurement of scattering parameters, which can also explain the phenomenon that the transmission magnitude is greater than 0 at low frequencies as shown in Fig. 3(a).

It can also be found from Fig. 3(a) that the transmission loss of the ideal differential 50-mm-long structure is smaller, which is reasonable as the loss caused by connection and soldering is reduced. At high frequencies, ripples can be clearly seen due to the resonance of straight lines. Here the transmission loss per unit length among these three cases is also compared, as displayed in Fig. 5. The result of the ideal differential 50-mm-long structure was obtained based on equation (20). It can be seen that the unit length transmission loss of the ideal differential 50-mm-long structure is the smallest. Because of the connection and soldering loss, the averaged transmission loss per unit length for the fabricated 50 mm and 100 mm long structure are not the same, and that of the 50-mm-long structure is larger.

By using the proposed method, the derived loss components of the ideal differential 50-mm-long UGCPW structure can be calculated [see Fig. 6(a)]. it is noticed that the radiation loss and the conductor loss only account for a small portion of the total loss, while the UGCPW structure loss mainly comes from the substrate dielectric loss, which increases as the frequency becomes larger. A polynomial curve fitting approach was applied to represent the frequency dependency of the total loss, which can reduce the curve oscillation shown in Fig. 5. The derived dielectric loss tangent is depicted in Fig. 6(b), indicating that the value is maintained at around 0.0213 in the range from 12 to 20 GHz. At frequencies lower than 12 GHz, the dielectric loss tangent value is gradually increasing, which is mainly due to the fact that the electrical length of the ideal differential 50-mm-long UGCPW structure becomes smaller. The difference between the derived dielectric loss tangent of 0.0213 and the value of 0.02 shown in the

TABLE 1. Comparison of selected methods for substrate permittivity characterization.

Ref.	Ref. MUT	Frequency Range (GHz)	$\Delta\varepsilon$	$\Delta \tan\delta$
[9]	FR4	0.5-10.5 (Discrete)	~0.07 (1.7%)	~0.003 (15%)
[28]	FR4	2.2-3.4	~0.86 (20%)	NA (20%)
[29]	FR4	2-12 (Discrete)	~0.06 (1.5%)	NA
[30]	Rogers RO3850/ RO3006/ RO3010	to 67	~0.1-0.5 (3%-8%)	~0.004-0.008 (100%-200%)
This work	FR4	to 20	**~0.03 (0.68%)**	**~0.0013 (6.5%)**

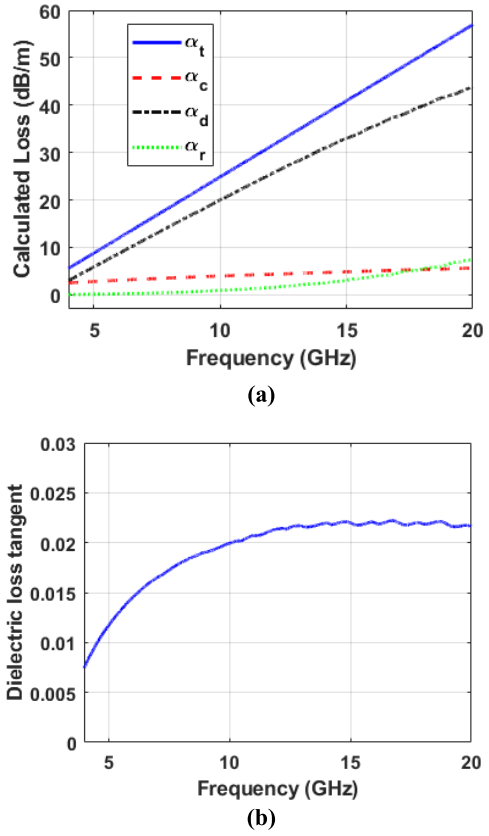

FIGURE 6. The derived (a) loss components of the ideal differential 50-mm-long UGCPW structure (total loss α_t, conductor loss α_c, dielectric loss α_d, radiation loss α_r), and (b) dielectric loss tangent of FR4 substrate material.

FR4 datasheet is 0.0013, i.e. 6.5%, which is more accurate than the error occurred in [9].

A comparison between the proposed approach and other methods reported in the literature is summarized in Table 1. Since SMA coaxial connectors are used, only the material properties at frequencies below 20 GHz are characterized in this work. As the proposed algorithm is based on the quasi-TEM approximation, the material characterization at higher frequencies is possible if the quasi-TEM wave assumption and good welding accuracy of millimeter-wave connectors, e.g. 2.92mm connectors, are satisfied. At higher frequencies, if the quasi-TEM approximation is no longer valid, the effective dielectric constant would show an obvious frequency dispersion. On the other hand, it is difficult to maintain the welding consistency, thereby, leading to larger error at higher frequencies. In this work, the proposed method was verified in the frequency range of interest below 20 GHz. Compared with the results presented in the literature, our proposed method can offer a more accurate retrieved complex dielectric permittivity, with an extraction error of the dielectric constant and dielectric loss tangent of only 0.68% and 6.5%, respectively. The slight deviations of the derived dielectric constant and dielectric loss tangent may be due to the non-perfectly identical connection and soldering of these two UGCPW structures. This is considered as the main source of the error, and it could be optimized with more advanced connection and soldering techniques. Furthermore, the calculation did not account for the metal surface treatment, where the immersion gold was applied to prevent the copper oxidation. Moreover, the error in fabrication and geometry of the UGCPW structures may cause errors in the derived dielectric properties as well, which could be improved by applying more accurate manufacturing methods. The proposed method can also be applied to other waveguide structures as well. When obtaining the differential phase and effective dielectric constant, substrate dielectric constant and dielectric loss tangent can be extracted by accurately separating all kinds of losses in combination with the structure dimensions.

IV. CONCLUSION

A novel method for fast determining broadband and continuous dielectric properties of substrate materials was presented in this paper. The derivation and optimization are based on the UGCPW structures containing two simple straight lines. The UGCPW configuration is suitable for electroplating certain newly developed dielectric materials, avoiding high fabrication cost and difficulty, as well as possible consistency error in conductor thickness and roughness caused by multiple electroplating process. In addition, the error caused by connector soldering and fabrication can be alleviated by jointly utilizing the scattering parameters of two straight lines. The loss components of the proposed structure and the cause of the deviation in the dielectric property have also been discussed. Based on the proposed method, the dielectric property of the widely used FR4 substrate has been characterized at frequencies below 20 GHz. The derived results show a good agreement with the values provided in the vendor's datasheet. The deviation of the derived dielectric constant and dielectric loss tangent are as small as 0.03 (0.68%) and 0.0013 (6.5%), respectively. Although the proposed approach is simpler than the WCM algorithm, the extraction accuracy is higher than the results reported in the literature since the conductor loss and radiation loss are taken into account during the retrieval process.

ACKNOWLEDGMENT

The authors would like to thank R. Mei for the help of manuscript proofreading.

REFERENCES

[1] S. Sahin, N. K. Nahar, and K. Sertel, "Permittivity and Loss Characterization of SUEX epoxy films for mmW and THz applications," *IEEE Trans. THz Sci. Technol.*, vol. 8, no. 4, pp. 397–402, Jul. 2018.

[2] N. Ghalichechian and K. Sertel, "Permittivity and loss characterization of SU-8 Films for mmW and Terahertz applications," *IEEE Antennas Wireless Propag. Lett.*, vol. 14, pp. 723–726, 2015.

[3] F. Declercq, H. Rogier, and C. Hertleer, "Permittivity and loss tangent characterization for garment antennas based on a new matrix-pencil two-line method," *IEEE Trans. Antennas Propag.*, vol. 56, no. 8, pp. 2548–2554, Aug. 2008.

[4] X. Lin and B.-C. Seet, "Dielectric characterization at millimeter waves with hybrid microstrip-line method," *IEEE Trans. Instrum. Meas.*, vol. 66, no. 11, pp. 3100–3102, Nov. 2017.

[5] R. Kumar, P. Kumar, N. Gupta, and R. Dubey, "Experimental investigations of wearable antenna on flexible perforated plastic substrate," *Microw. Opt. Technol. Lett.*, vol. 59, no. 2, pp. 265–270, Feb. 2017.
[6] I. Maestrojuan, I. Palacios, I. Ederra, and R. Gonzalo, "USE of COC substrates for millimeter-wave devices," *Microw. Opt. Technol. Lett.*, vol. 57, no. 2, pp. 371–377, Feb. 2015.
[7] R.-Y. Yang, Y.-K. Su, M.-H. Weng, C.-Y. Hung, and H.-W. Wu, "Characteristics of coplanar waveguide on lithium niobate crystals as a microwave substrate," *J. Appl. Phys.*, vol. 101, no. 1, Jan. 2007, Art. no. 014101.
[8] C.-L. Yang, C.-S. Lee, K.-W. Chen, and K.-Z. Chen, "Noncontact measurement of complex permittivity and thickness by using planar resonators," *IEEE Trans. Microw. Theory Techn.*, vol. 64, no. 1, pp. 247–257, Jan. 2016.
[9] K.-P. Latti, M. Kettunen, J.-P. Strom, and P. Silventoinen, "A review of microstrip T-resonator method in determining the dielectric properties of printed circuit board materials," *IEEE Trans. Instrum. Meas.*, vol. 56, no. 5, pp. 1845–1850, Oct. 2007.
[10] A. A. Takach, F. M. Moukanda, F. Ndagijimana, M. Al-Husseini, and J. Jomaah, "Two-line technique for dielectric material characterization with application in 3D-printing filament electrical parameters extraction," *Prog. Electromagn. Res. M*, vol. 85, pp. 195–207, Oct. 2019.
[11] M. H. Hosseini, H. Heidar, and M. H. Shams, "Wideband nondestructive measurement of complex permittivity and permeability using coupled coaxial probes," *IEEE Trans. Instrum. Meas.*, vol. 66, no. 1, pp. 148–157, Jan. 2017.
[12] L. Cai, H. Xu, and D. Chu, "Compact liquid crystal based tunable band-stop filter with an ultra-wide stopband by using wave interference technique," *Int. J. Antennas Propag.*, vol. 2017, pp. 1–11, Feb. 2017.
[13] L. A. Benali, A. Tribak, J. Terhzaz, and A. Mediavilla, "Estimation of the complex permittivity of a bi-layer dielectric material in X-band frequencies," in *Proc. 2nd Int. Conf. Comput. Wireless Commun. Syst. (ICCWCS)*, 2017, p. 35.
[14] L. Cai and D. Chu, "Highly anisotropic LC material with low dielectric loss for the application of tunable notch filters," *J. Electromagn. Waves Appl.*, vol. 33, no. 8, pp. 1070–1081, May 2019.
[15] L. Cai, H. Xu, J. Li, and D. Chu, "High figure-of-merit compact phase shifters based on liquid crystal material for 1–10 GHz applications," *Jpn. J. Appl. Phys.*, vol. 56, no. 1, Jan. 2017, Art. no. 011701.
[16] R. Dib, D. Vincent, and A. Elrafhi, "Measurement of the electromagnetic properties of thin-films using a microwave resonant cavity," *Microw Opt Technol Lett*, vol. 61, no. 1, pp. 15–19, Jan. 2019.
[17] L.-F. Chen, C. K. Ong, C. P. Neo, V. V. Varadan, and V. K. Varadan, *Microwave Electronics: Measurement and Materials Characterization*. Hoboken, NJ, USA: Wiley, 2004.
[18] X.-C. Zhu, W. Hong, P.-P. Zhang, Z.-C. Hao, H.-J. Tang, K. Gong, J.-X. Chen, and K. Wu, "Extraction of dielectric and rough conductor loss of printed circuit board using differential method at microwave frequencies," *IEEE Trans. Microw. Theory Techn.*, vol. 63, no. 2, pp. 494–503, Feb. 2015.
[19] D. E. Zelenchuk, V. Fusco, G. Goussetis, A. Mendez, and D. Linton, "Millimeter-wave printed circuit board characterization using substrate integrated waveguide resonators," *IEEE Trans. Microw. Theory Techn.*, vol. 60, no. 10, pp. 3300–3308, Oct. 2012.
[20] R. Marks, "A multiline method of network analyzer calibration," *IEEE Trans. Microw. Theory Techn.*, vol. 39, no. 7, pp. 1205–1215, Jul. 1991.
[21] C. Wan, B. Nauwelaers, and W. De Raedt, "A simple error correction method for two-port transmission parameter measurement," *IEEE Microw. Guided Wave Lett.*, vol. MGWL-8, no. 2, pp. 58–59, Feb. 1998.
[22] S. Can, K. Y. Kapusuz, and A. E. Yilmaz, "Optically transparent frequency selective surface for ultrawideband applications," *Microw. Opt. Technol. Lett.*, vol. 59, no. 12, pp. 3197–3201, Dec. 2017.
[23] U. C. Hasar, G. Buldu, M. Bute, J. J. Barroso, T. Karacali, and M. Ertugrul, "Determination of constitutive parameters of homogeneous metamaterial slabs by a novel calibration-independent method," *AIP Adv.*, vol. 4, no. 10, Oct. 2014, Art. no. 107116.
[24] R. E. Collin, *Foundations for Microwave Engineering*. New York, NY, USA: Wiley, 2001.
[25] J. Carroll, M. Li, and K. Chang, "New technique to measure transmission line attenuation," *IEEE Trans. Microw. Theory Techn.*, vol. 43, no. 1, pp. 219–222, 1st Quart., 1995.
[26] J.-M. Heinola, K.-P. Latti, J.-P. Strom, M. Kettunen, and P. Silventoinen, "A strip line ring resonator method for determination of dielectric properties of printed circuit board material in function of frequency," in *Proc. 17th Annu. Meeting IEEE Lasers Electro-Opt. Soc. (LEOS)*, Dec. 2004, pp. 692–695.
[27] M. Riaziat, R. Majidi-Ahy, and I.-J. Feng, "Propagation modes and dispersion characteristics of coplanar waveguides," *IEEE Trans. Microw. Theory Techn.*, vol. 38, no. 3, pp. 245–251, Mar. 1990.
[28] H. Shwaykani, A. El-Hajj, J. Costantine, F. A. Asadallah, and M. Al-Husseini, "Dielectric spectroscopy for planar materials using guided and unguided electromagnetic waves," in *Proc. IEEE Middle East North Africa Commun. Conf. (MENACOMM)*, Apr. 2018, pp. 1–5.
[29] E. Holzman, "Wideband measurement of the dielectric constant of an FR4 substrate using a parallel-coupled microstrip resonator," *IEEE Trans. Microw. Theory Techn.*, vol. 54, no. 7, pp. 3127–3130, Jul. 2006.
[30] P. Seiler and D. Plettemeier, "A method for substrate permittivity and dielectric loss characterization up to subterahertz frequencies," *IEEE Trans. Microw. Theory Techn.*, vol. 67, no. 4, pp. 1640–1651, Apr. 2019.

LONGZHU CAI (Member, IEEE) received the B.Eng. degree from the Huazhong University of Science and Technology, Wuhan, China, and the University of Birmingham, Birmingham, U.K., in 2012, and the M.Res. and Ph.D. degrees from the University of Cambridge, Cambridge, U.K., in 2013 and 2017, respectively.

In 2017, he joined the School of Information Science and Engineering, Southeast University, Nanjing, China. His current research interests include microwave (MW) component designs, study of smart materials, and the development of liquid crystal as a tunable dielectric for MW applications.

ZHI HAO JIANG (Member, IEEE) was born in Nanjing, China, in 1986. He received the B.S. degree in radio engineering from Southeast University, Nanjing, in 2008, and the Ph.D. degree in electrical engineering from The Pennsylvania State University at University Park, State College, PA, USA, in 2013.

From 2013 to 2016, he was a Postdoctoral Fellow with the Computational Electromagnetics and Antennas Research Laboratory, Department of Electrical Engineering, The Pennsylvania State University. He is currently a Professor with the State Key Laboratory of Millimeter Waves, School of Information Science and Engineering, Southeast University. He has authored or coauthored about 80 articles in peer-reviewed journals, over 70 papers in conference proceedings, and eight book chapters. He has also co-edited one book *Electromagnetics of Body Area Networks: Antennas, Propagation, and RF Systems* (Wiley/IEEE Press, 2016). He holds seven granted U.S. patents and one granted Chinese patent. He has served as the TPC Co-Chair or a TPC Member for multiple international conferences. He was a recipient of the Young Scientist Award at the 2019 ACES-China Conference, the High-Level Innovative and Entrepreneurial Talent presented by Jiangsu Province, China, in 2017, the Thousands of Young Talents presented by the China Government, in 2016, the Honorable Mention at the IEEE AP-S International Symposium on Antennas and Propagation Student Paper Contest, in 2013, and the 2012 A. J. Ferraro Outstanding Doctoral Research Award in Electromagnetics. He serves as an Associate Editor for *IET Communications* and a reviewer for more than 40 journals. He served as a Guest Editor for the *International Journal of RF and Microwave Computer-Aided Engineering*. His current research interests include microwave/millimeter-wave antennas and circuits, millimeter-wave systems, impedance surfaces, metamaterials, and analytical methods.

YAN HUANG (Member, IEEE) received the B.S. degree in electrical engineering and the Ph.D. degree in signal and information processing from Xidian University, Xi'an, China, in 2013 and 2018, respectively.

He was a Visiting Ph.D. Student with the Electrical and Computer Engineering Department, University of Florida, Gainesville, FL, USA, from 2016 to 2017, and the Electrical and Systems Engineering Department, Washington University in St. Louis, St. Louis, MO, USA, from 2017 to 2018. He is currently an Assistant Professor with the State Key Laboratory of Millimeter Waves, Southeast University, Nanjing, China. His research interests include machine learning, synthetic aperture radar, image processing, and ground moving target indication.

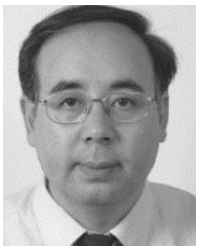

WEI HONG (Fellow, IEEE) received the B.S. degree in radio engineering from the University of Information Engineering, Zhengzhou, China, in 1982, and the M.S. and Ph.D. degrees in radio engineering from Southeast University, Nanjing, China, in 1985 and 1988, respectively.

In 1993, he joined the University of California at Berkeley, Berkeley, CA, USA, as a short-term Visiting Scholar. From 1995 to 1998, he was a short-term Visiting Scholar with the University of California at Santa Cruz, Santa Cruz, CA, USA. Since 1988, he has been with the State Key Laboratory of Millimeter Waves, Southeast University, where he has been the Director, since 2003. He is currently a Professor and the Dean of the School of Information Science and Engineering. He is also involved in numerical methods for electromagnetic problems, millimeter-wave theory and technology, antennas, and RF technology for wireless communications. He has authored or coauthored over 300 technical publications with over 9000 citations and has authored two books. He was an Elected IEEE MTT-S Ad Com Member, from 2014 to 2016. He is a Fellow of CIE. He was twice awarded the National Natural Prizes and thrice awarded the First-Class Science and Technology Progress Prizes issued by the Ministry of Education of China and the Jiangsu Province Government. He also received the Foundations for China Distinguished Young Investigators and for Innovation Group issued by NSF of China. He is the Vice President of the CIE Microwave Society and the Antenna Society and the Chair of the IEEE MTT-S/AP-S/EMC-S Joint Nanjing Chapter. He served as an Associate Editor for the IEEE TRANSACTIONS ON MICROWAVE THEORY AND TECHNIQUES, from 2007 to 2010. He was one of the guest editors of the 5G Special Issue of the IEEE TRANSACTIONS ON ANTENNAS AND PROPAGATION, in 2017.